NASA/TM-1998-206566

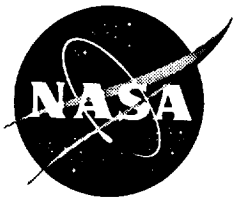

An Overview of an Experimental Demonstration Aerotow Program

James E. Murray, Albion H. Bowers, William A. Lokos, Todd L. Peters
Dryden Flight Research Center
Edwards, California

Joseph Gera
Analytical Services and Materials, Inc.
Edwards, California

National Aeronautics and
Space Administration

Dryden Flight Research Center
Edwards, California 93523-0273

September 1998

NOTICE

Use of trade names or names of manufacturers in this document does not constitute an official endorsement of such products or manufacturers, either expressed or implied, by the National Aeronautics and Space Administration.

Available from the following:

NASA Center for AeroSpace Information (CASI)
7121 Standard Drive
Hanover, MD 21076-1320
(301) 621-0390

National Technical Information Service (NTIS)
5285 Port Royal Road
Springfield, VA 22161-2171
(703) 487-4650

AN OVERVIEW OF AN EXPERIMENTAL DEMONSTRATION AEROTOW PROGRAM

James E. Murray,* Albion H. Bowers,† William A. Lokos,‡ Todd L. Peters§
NASA Dryden Flight Research Center
Edwards, California
Joseph Gera,¶
Analytical Services and Materials, Inc.
Edwards, California

Abstract

An overview of an experimental demonstration of aerotowing a delta-wing airplane with low-aspect ratio and relatively high wing loading is presented. Aerotowing of future space launch configurations is a new concept, and the objective of the work described herein is to demonstrate the aerotow operation using an airplane configuration similar to conceptual space launch vehicles. Background information on the use of aerotow for a space launch vehicle is presented, and the aerotow system used in this demonstration is described. The ground tests, analytical studies, and flight planning used to predict system behavior and to enhance flight safety are detailed. The instrumentation suite and flight test maneuvers flown are discussed, preliminary performance is assessed, and flight test results are compared with the preflight predictions.

Nomenclature

DGPS	differentially-corrected global positioning system
KCAS	knots calibrated airspeed
KST	Kelly Space and Technology, San Bernardino, California
psi	pounds per square inch
ΔL	change in towrope length, ft
$\dot{\Delta L}$	rate of change in towrope length, ft/sec

*James E. Murray, Aerospace Engineer, Aerodynamics Branch, (805) 258-2629, murray@rigel.dfrc.nasa.gov
†Albion H. Bowers, Aerospace Engineer, Aerodynamics Branch, (805) 258-3716, bowers@orville.dfrc.nasa.gov
‡William A. Lokos, Aerospace Engineer, Aerostructures Branch, (805) 258-3924, Bill.Lokos@dfrc.nasa.gov
§Todd L. Peters, Flight Loads Engineer, Aerostructures Branch, (805) 258-2843, Todd.Peters@dfrc.nasa.gov
¶Joseph Gera, Engineer, Analytical Services and Materials, Inc., (805) 258-7917, Joe.Gera@dfrc.nasa.gov

Introduction

The concept of aerotowing is an old one, first proposed by Anthony Fokker of the Netherlands during World War I. It was later made practical in Germany, principally for the launching of sailplanes (ref. 1). In succeeding years, a wide variety of aerotow configurations have been flown, including a rocket-powered tailless fighter (ref. 2), a propeller-driven fighter (ref. 3), a jet-powered fighter (ref. 4), and a lifting body (ref. 5). While aerotow is practiced widely today as a sailplane launch method (ref. 6), flight-validated modeling of the aerotow configuration is still immature. Much useful theoretical work has been reported (refs. 7–15), but comparisons with flight results are largely qualitative and anecdotal.

In the early 1990s, Kelly Space & Technology (KST), (San Bernardino, California), proposed and patented the use of aerotow as part of a low-cost method for launching satellites into a low Earth orbit (ref. 16). The United States Air Force Research Laboratory (Kirtland Air Force Base, New Mexico) supported KST to study and demonstrate the feasibility of aerotow with aircraft that were more representative of this type of space launch system. The KST space launch concept (fig. 1) makes use of a transport category aircraft as a tow plane, and a space launch rocket being towed. For this demonstration, the USAF Air Force Flight Test Center, Edwards, California, provided use of a C-141A Starlifter aircraft (Lockheed Aircraft Corporation, Burbank, California) as a representative transport category aircraft. The United States Air Force Research Laboratory also arranged the loan to National Aeronautics and Space Administration of two QF-106A Delta Dart aircraft (Convair Division of General Dynamics, San Diego, California) to use for the flight program. The flight test program was conducted by the NASA Dryden Flight Research Center and the U.S. Air Force Flight Test Center at Edwards Air Force Base, Edwards, California.

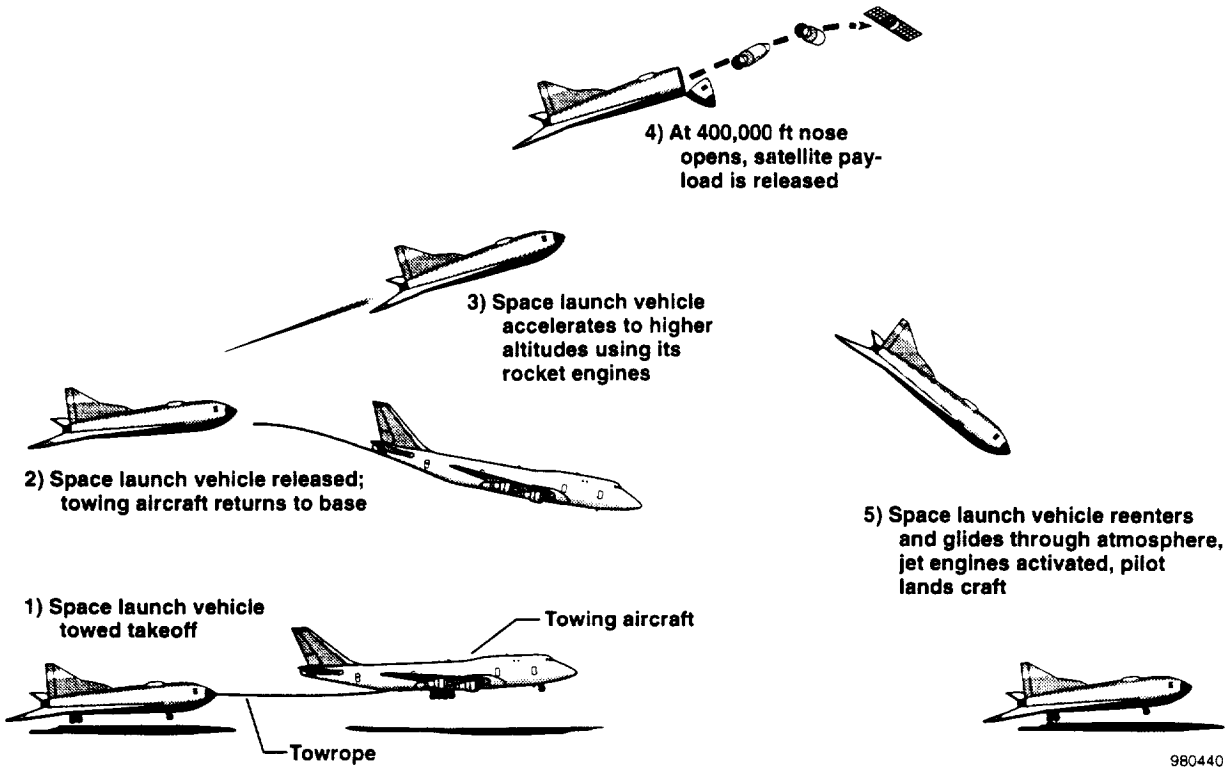

Figure 1. Aerotow space launch concept schematic.

This paper provides an overview of a flight demonstration of the aerotow system. The paper also describes the aerotow system used in the flight program, including (1) the modifications to the test aircraft, (2) the ground testing and analytical studies used to validate the structural integrity of the system design, and (3) the analytical studies used to predict the characteristics of the aerotow system. Details of the research instrumentation system that was installed to collect flight data for validation of the preflight predictions are presented. The operational aspects of the flight test program and the research maneuvers flown are described, and selected flight results are presented and compared with the preflight predictions.

Use of trade names or names of manufacturers in this document does not constitute an official endorsement of such products or manufacturers, either expressed or implied, by the National Aeronautics and Space Administration.

Aerotow System Description

The complete aerotow system (fig. 2) consists of three distinct subsystems: the towing aircraft, the towed aircraft, and the interconnecting tow train. Configuration of each subsystem is discussed separately.

Towing Aircraft

The C-141A Starlifter, hereinafter referred to as the towing aircraft, (fig. 3) is a transport category military aircraft. It has a swept wing which is shoulder mounted on the fuselage, a large "T" tail, and four high-bypass turbofan engines. The takeoff weight for towed operation was nominally 200,000 lb to maximize takeoff performance. The standard C-141A has a large cargo door and loading ramp at the aft end of the fuselage, and a pressure bulkhead door which is normally closed in cruise flight to allow pressurization of the cargo area. For the aerotow program the towing aircraft was configured with the cargo door removed, the loading ramp up and locked, the pressure door open, and a test pallet with ballast locked at the aft end of the cargo bay. The aft end of the pallet was equipped with an integral mandrel and manually-operated redundant guillotine assembly for single-point load attachment and release capability.

EC98-44415-19

Figure 2. Aerotow system in flight.

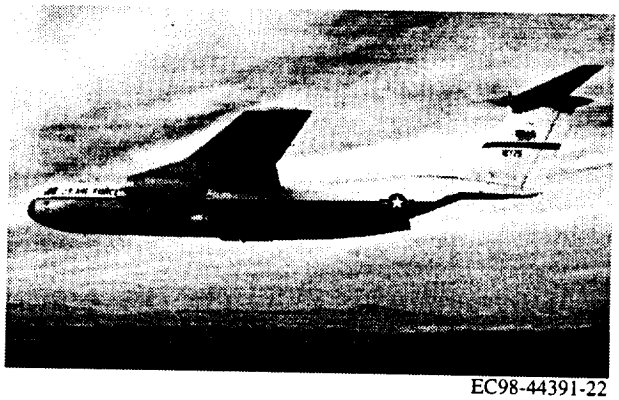

EC98-44391-22

Figure 3. C-141A towing aircraft in flight.

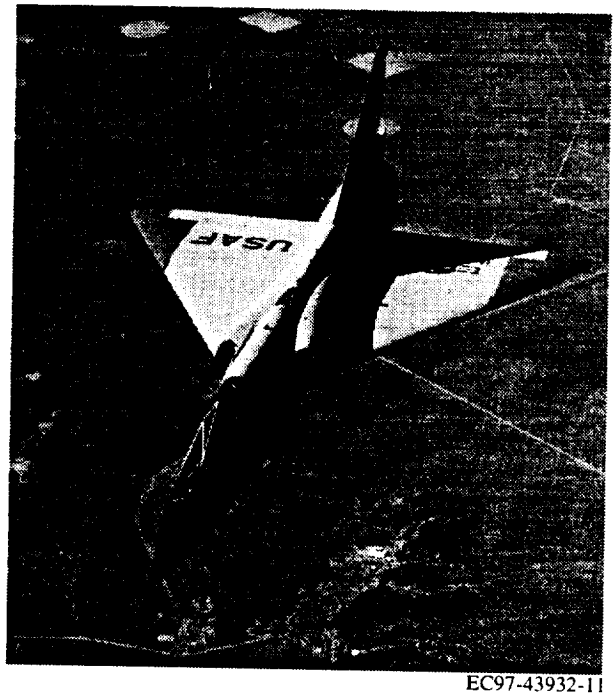

EC97-43932-11

Figure 4. QF-106A towed aircraft in flight.

Towed Aircraft

The QF-106A Delta Dart aircraft, hereinafter referred to as the towed aircraft, (fig. 4) was originally designed as an interceptor aircraft with Mach 2+ capability. It has a delta wing mounted low on the fuselage and a single engine buried in the fuselage. The takeoff weight for towed operations was nominally 30,300 lb.

Design Philosophy

The towed aircraft was modified to enable towing by means of a nose-mounted tow mechanism. Needless to say there was no consideration given to this possibility during the original design effort 40 years before! Fortunately the forward fuselage was designed to support the inertial loads of relatively large and heavy RADAR and infrared search and track systems. As the

aerotow demonstration did not require the full load factor envelope of the aircraft, considerable excess structure in the forward fuselage was available to carry the majority of the tow loads. To reduce possible interference with the towrope the airdata noseboom was shortened by 50 in. and recalibrated prior to towed flight operations.

Confidence in the design loads was gained through simulation, which had established the expected tow load envelope and magnitude. A ±20° tow cone angle, with respect to aircraft body axes, and a magnitude of 24,000 lb were selected for design purposes. A well-tested frangible link was included in the tow load path to ensure that the maximum tow load applied to the aircraft would never exceed 24,000 lb.

Confidence in the strength of the structural system was gained through stress analyses and component testing. All new and modified structure was treated as primary structure. Frangible link failure load (a nominal 24,000 lb) established the design limit load. All new and modified structure was designed for a factor of safety of 2.25 times the design limit load for the specified towrope cone angle. There was no need to pursue a minimum weight solution to the design requirements, and redundancy was used whenever possible.

Weldment and Release Mechanism

Tow loads were transferred into the airframe through a release mechanism attached to a custom weldment attached to the upper fuselage just forward of the windscreen (fig. 5). The release mechanism was a standard B-52 landing drag parachute mechanism. To make the interface between the tow train and the release mechanism functionally identical to the B-52 installation, a restraint block was added just forward of the release hook. The electro-pneumatic actuation system, originally used for the infrared search and track system, was retained and modified to actuate the release mechanism. This primary tow train release system was initiated by a button on the pilot's control stick, and was backed up with a manually-operated release T-handle installed in the cockpit.

Structural Reinforcement

The fuselage skin was reinforced in several areas. Six 0.040-inch-thick 2024 aluminum skin doublers were installed on the forward fuselage. These sheet metal modifications helped to distribute tensile load and to bridge a major fuselage assembly joint, which otherwise might not have had adequate strength. Two 0.125-inch-thick 321 stainless steel skin doublers were installed on the fuselage sides to reinforce the intersection of key longerons. Inspection hole covers in the forward fuselage were replaced with hole doublers for easy access inspection. Left and right gussets were installed in the forward fuselage.

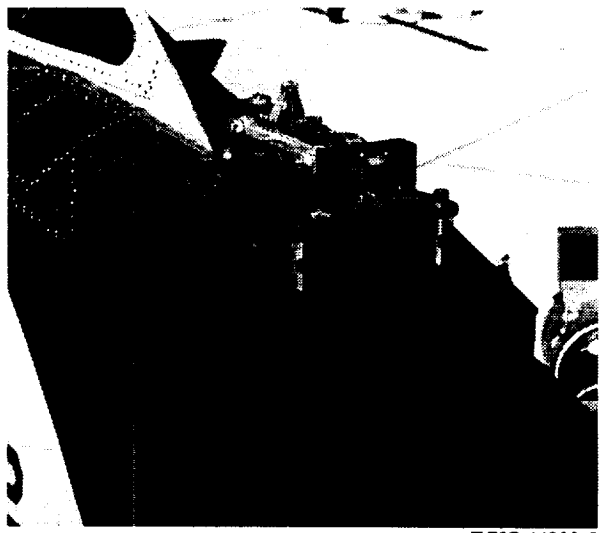

EC97-44233-5

Figure 5. Weldment and release mechanism installed on towed aircraft.

Cockpit

The tactical display, wind screen divider, accelerometer, and compass were removed for increased visibility. The forward cockpit bulkhead was penetrated to install the manual release cable and two electrical connectors. Towrope tension displays and the manual rope release handle were installed in a new panel, replacing the tactical display.

Tow Train

The tow train assembly that connected the two aircraft is shown schematically in figure 6. Two configurations were used. The following description is for the initial configuration (fig. 6(a)) and begins at the towing aircraft guillotine mandrel and ends at the towed aircraft release mechanism; the later configuration (fig. 6(b)) is a simplification of the initial configuration.

A 1.75-inch-wide eight-ply nylon strap was wrapped over the guillotine mandrel. The nylon allowed the blades of the guillotine to sever the tow train so it could be dropped prior to landing the towing aircraft. The nylon strap was attached to a three-pin connector, which was used to allow rapid assembly of the tow train when attaching it to the towing aircraft on the runway.

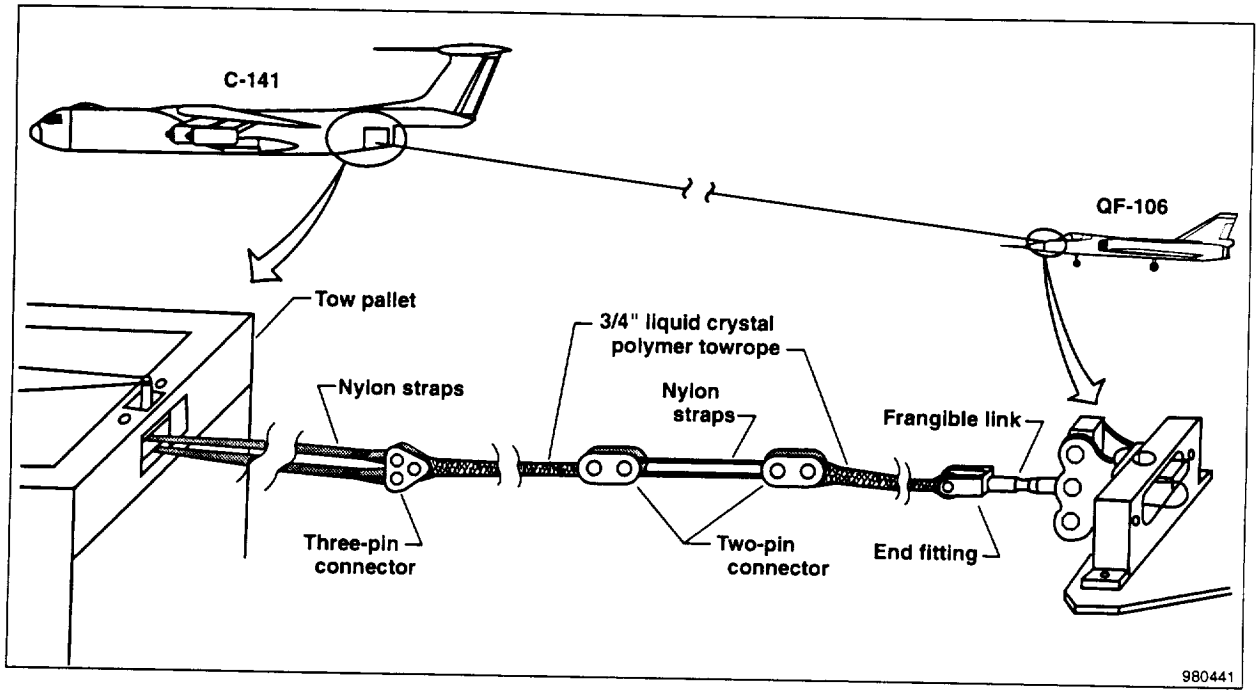

(a) Initial configuration.

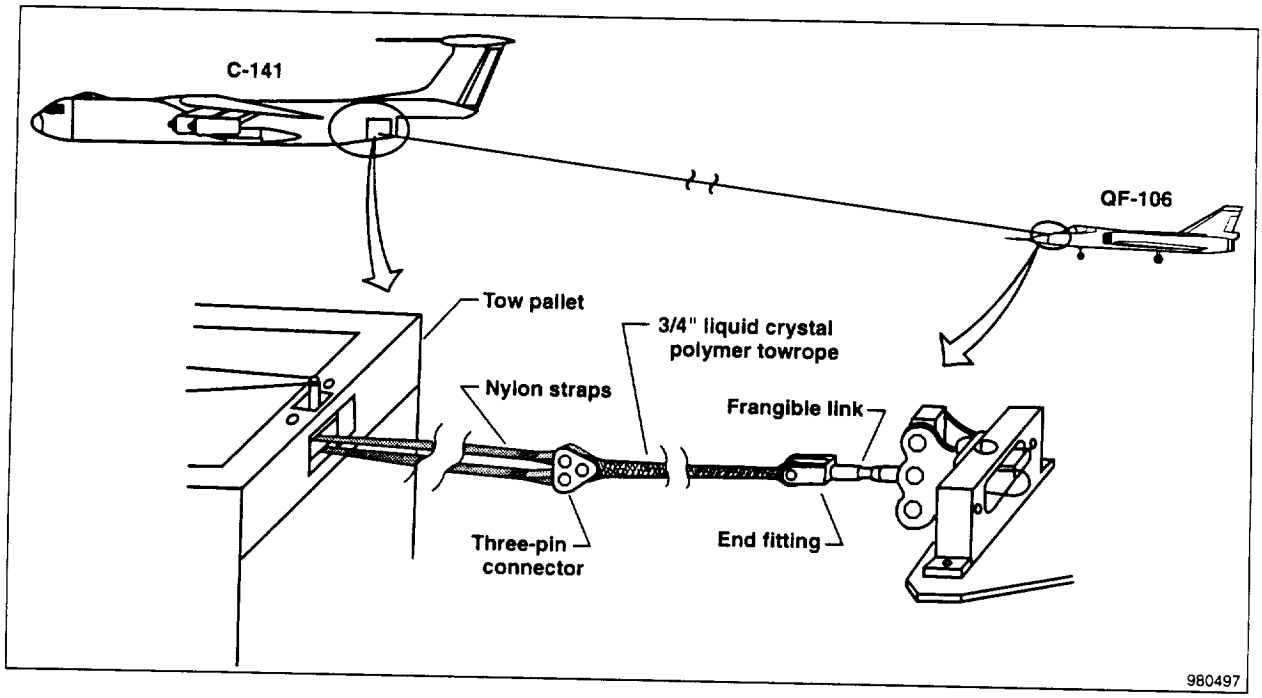

(b) Simplified configuration.

Figure 6. Schematic drawing of tow train assembly.

Attached to the aft end of the three-pin connector was a 500-foot length of 0.75-inch-diameter liquid crystal polymer towrope. The forward end of the towrope was braided into a 10-foot-long loop with a double interlocking splice. The long loop was made so that a double strand of the towrope would extend across the edge of the towing aircraft ramp. The aft end of the forward section of towrope was braided into a 1-foot-long loop with a double interlocking splice and connected to a 50-foot length of eight-ply 1.75-inch-wide nylon strap with a two-pin connector. The nylon strap was followed by another two-pin connector which was connected to another 500-foot-long section of rope. This center section of nylon was added to provide damping to the tow train system during the high-speed taxi test, and was used in the first two aerotow demonstration flights. The nylon damper assembly was protected from abrasion while contacting the runway by a heavy canvas cover that extended over both two-pin connectors and was secured at the forward two-pin connector. The canvas cover was allowed to float over the aft two-pin connector. For the second configuration, this entire segment of two-pin connector, nylon damper assembly, and two-pin connector was deleted and a continuous 1000-foot-long towrope was used (fig. 6(b)).

At the aft end of the towrope the final splice loop was made through a steel end-fitting, which was threaded onto a frangible link. The frangible link was in turn threaded to an adapter, which was bolted to a stock B-52 drag parachute assembly that consisted of a riser fitting, a universal joint, and a D-ring. This assembly plugged into the restraint block and release mechanism (also stock B-52 hardware) attached to the weldment. Transducers on the frangible link and the universal joint were connected to the aircraft instrumentation system with an electrical quick-disconnect.

Ground Testing

As part of the structural safety-of-flight effort, considerable ground proof and functional testing of individual components and assemblies were performed. These test articles included the frangible links, the liquid crystal polymer towrope, the nylon strap, the towed aircraft release mechanism, and the towing aircraft guillotine mechanism. Several tow train components such as the three-pin connectors and the adapters were never proof-tested to failure because they were designed to a factor of safety of 2.25 or more.

Frangible Links

The three functions of the frangible link were as follows: (1) to limit the peak tow train load to a nominal 24,000 lb, (2) to fix the location of any tow train break, and (3) to give a real-time measurement of the tow load. In order to retrofit the original link design to incorporate the load measurement feature a parametric study was undertaken to show the effect of link length on the resolution of the available load signal. Three links of different lengths (fig. 7) were fabricated and instrumented with prime and spare dual-tee strain gage bridges. Each strain gage bridge was calibrated within the elastic range. The data were linear and showed that within the range of length variation studied there was no significant effect on resolution and that the proposed strain gage configuration would be sufficient for the intended purpose.

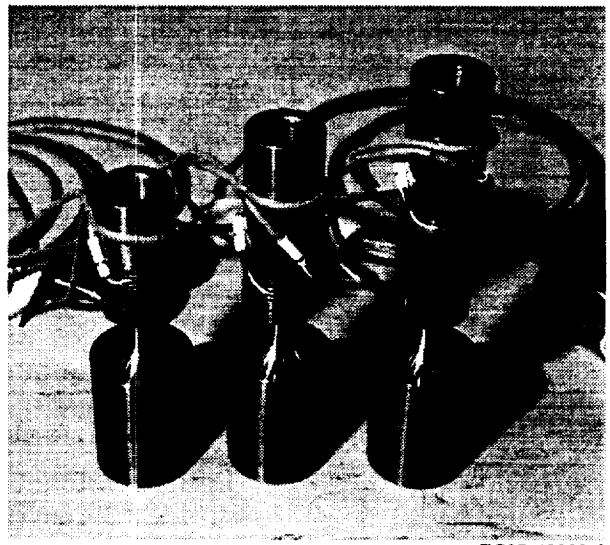

EC97-43899-3

Figure 7. Developmental frangible links.

In order to achieve uniform through-hardening the frangible link metal stock was specified to be 4340 alloy steel. The metal was heat treated to a nominal 125,000 psi; however initial developmental proof tests indicated that the actual material strength was closer to 150,000 psi, which led to a slight design change in neck diameter. The neck of the frangible link was designed to a factor of safety of 1.00 while the rest of the frangible link design was good for at least 2.25 times the design limit load. For the flight batch, nineteen links were machined from the same piece of bar stock. Of these, ten were set aside for flight use and nine were proof-tested to failure. These nine proof tests indicated excellent repeatability and provided confidence in the fuse precision of the flight items. The ten flight links were instrumented and calibrated through their elastic range. Because the strain gages were located on the shoulder of

the design and not on the neck they were able to provide linear results all the way to frangible-link failure in the case of flight overload. The dual-tee strain gage bridge configuration provided good output for tensile loads and self-correction for temperature effects and any incidental bending loads.

Towrope Assembly

The towrope was a crucial element in the tow train and was tested extensively to establish confidence in its characteristics. Cyclical loading was used to determine the stiffness and damping characteristics of the rope. This information was essential to building a good system dynamic simulation. Proof-test to failure under optimum conditions was used to confirm the maximum strength of the rope. High-cycle loading followed by proof-test to failure was used to evaluate the fatigue strength. Cyclical loading with the rope bent over a fixed mandrel followed by proof-test to failure was used to evaluate wear characteristics. An artificially abraded test rope was proof tested, to show the residual strength of an extremely worn rope. All of this testing showed that the towrope selected was relatively stiff, had relatively little damping, had a maximum strength of more than 2.25 times the design limit load, excellent wear resistance, and a residual strength close to 1.5 times the design limit load after extreme abrasion or four-times-life-cycle fatigue loading. Samples of nylon strap were also tested for ultimate strength, stiffness, wear resistance and damping.

Towrope end loop splices were woven by hand and were considered a critical component of the tow train assembly load path, so were scrutinized for adequacy. Six test specimens were prepared and tested to failure. In each case the rope itself failed and the end loops held. All flight rope end loops were fabricated by the same technician using the same process. No end loop splice ever failed during any of the ground or flight tests.

Towed Aircraft Release Mechanism

This release mechanism was originally a B-52 drag parachute release and was qualified for strength based on similarity to identical mechanisms which have been operated at loads well in excess of the system design ultimate strength of 54,000 lb, therefore no proof test was required. This mechanism was tested under varied axial loads to quantify the corresponding required actuation force. The release actuation system was designed to provide several times the typical 30 lbf required to assure reliable rope-release capability. This release mechanism, in combination with the restraint block, was subjected to a series of release functional tests at rope loads up to 24,000 lb and at off-axis rope angles up to 20° azimuth and elevation (fig. 8) to verify reliable operation throughout the functional design envelope. However, if the load was below 2000 lb, the universal joint assembly did not aggressively exit the release mechanism when commanded. Therefore, the minimum rope tension criterion for release during flight was set at a nominal 3,000 lb to ensure clean separation of the assembly from the towed aircraft.

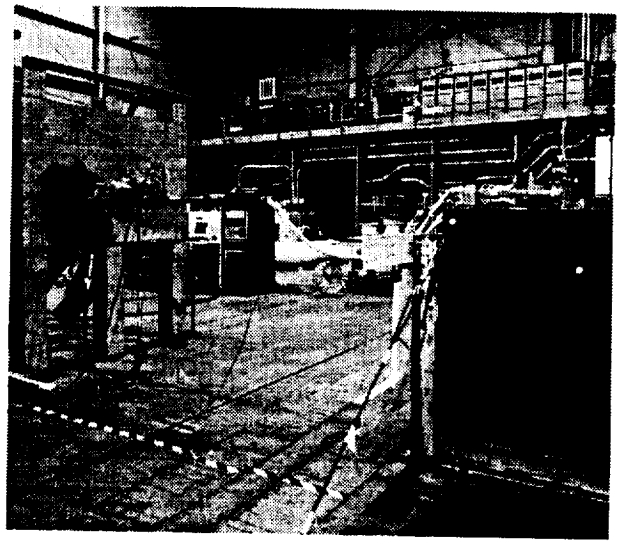

EC97-44162-5

Figure 8. Loaded release test setup.

Towing Aircraft Release Guillotine

Functional testing of the tow release guillotine was performed to verify reliability. Both towrope and multiple layers of 1.75-inch-wide nylon strap were experimented with. Neither the prime nor backup cutter could completely sever the liquid crystal polymer towrope. As a result an absolute requirement to use nylon at the front of the tow train was incorporated. Multiple layers of nylon could be cut if the blades were kept sharp and care was taken during rigging to keep the straps centered on the mandrel.

Loaded Angle Calibration

The universal joint was instrumented in both azimuth and elevation angles for tension vector decomposition and to support real-time monitoring of the rope angle with respect to its design envelope. Each universal joint assembly was calibrated under load to eliminate free play and to replicate the in-flight load environment.

Canopy Stiffness Test

During the design process, consideration was given to the possible consequences of twisting and bending the fuselage in new and different ways through the application of tow loads. A concern developed that this could interfere with proper functioning of the emergency egress system. Finite element analysis of the forward fuselage deflection under the worst-case tow load indicated that the spacing between the left and right canopy rails could be elastically reduced by as much as one-eighth of an inch. The question was whether there could be enough binding produced to inhibit canopy jettison. Having no finite element model of the canopy, it was decided to test its stiffness to show how much side force on the canopy would be required to produce the predicted deflection of the mating fuselage structure. A simple deadweight loading test was performed using shot bags and a spare canopy as shown in figure 9. The test results indicated that the potential binding force was small in comparison to the available pyrotechnic jettison force and that the risk of binding at a critical moment was not significantly increased by tow loads.

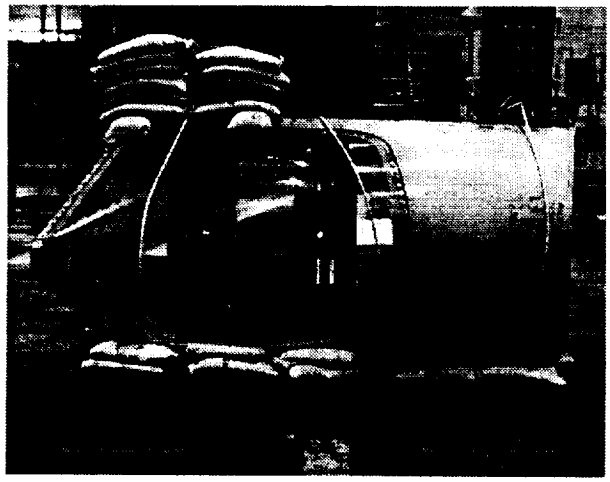

EC97-44303-1

Figure 9. Canopy stiffness test setup.

Tow Train Qualification

Prior to flight use, each tow train assembly was laid out on a taxiway and qualification load tested to 28,000 lb as a final form of inspection. A high-strength test link was substituted in the assembly for the flight frangible link. No failures occurred during these tests. This final ground test proved to be cheap insurance that no critical cuts or flaws existed in the 1,000-foot-long assembly.

Analytical Background

Analytical techniques were used extensively to augment and support the ground testing effort and to gain confidence in the towed system and operational procedures. Comprehensive structural modeling of the forward fuselage of the towed aircraft supported the mechanical design and modification effort. Piloted and batch simulations were developed and used to study towed system characteristics and to guide operational procedure development.

Structural Modeling

Analysis was the principal means of ensuring the structural integrity of the modified airframe with the expected tow loads. In conjunction with KST, a finite-element model of the forward fuselage of the towed aircraft (fig. 10) was developed to identify and quantify critical stress concentrations and distributions and to identify and quantify loads through critical joints. Furthermore, the model was used to quantify the canopy rail deflections and to suggest the required structural modifications.

Essentially, there were two issues. The primary concern was that the original aircraft structure might need reinforcement in order to handle the applied tow loads. A secondary concern was that the canopy rails might undergo excessive deflection and impede canopy jettison.

An effort was made to deliver the model for minimum cost and in minimum time, by using linear analysis techniques and conservative structural modeling. Conservative material and element properties were used in areas where production drawings were not available. Worst-case loads predicted by extensive flight simulator work were used in the analysis.

As a result of the analysis, a number of areas in the forward fuselage were identified as high stress or low stiffness and reinforced as described in the Aerotow System Description section. Deflection analysis of the canopy rails, in conjunction with the canopy deflection ground test described in the Ground Testing section, showed that canopy jettison would not be impeded. Overall, the finite-element analysis, in conjunction with hand analysis, proved to be an invaluable tool to the program, and was instrumental in determining that the towed aircraft was flight ready.

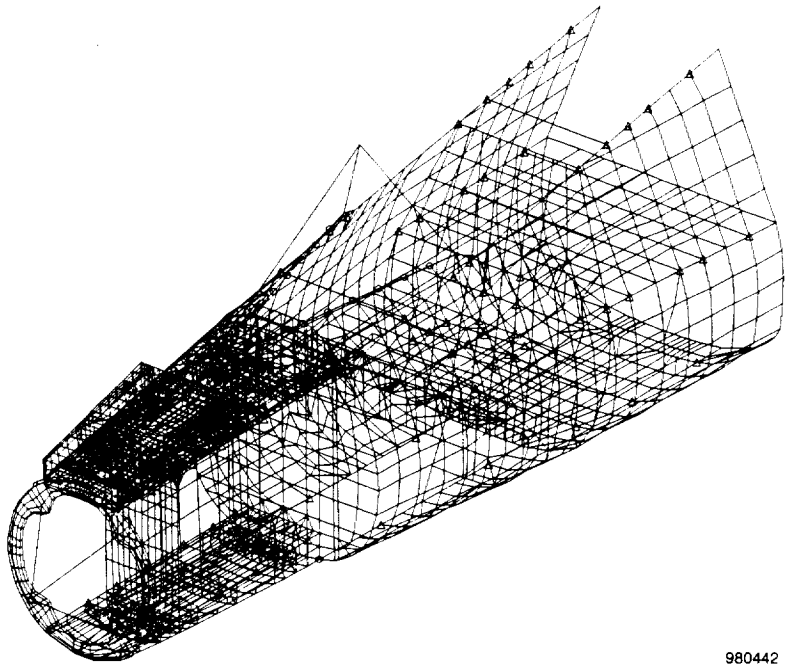

Figure 10. Towed aircraft forward fuselage finite element model.

Simulations

To enhance flight safety and to gain a better understanding of the coupled system dynamics the towed test flights were preceded by extensive simulations. In this section the simulation and the simplifying assumptions used in formulating the mathematical model are described. The dynamics of a physical system consisting of two aircraft connected by a towrope can be complex. The simulation model was simplified when possible, based on the results of preparatory untethered flight tests. Initial tow positions were arrived at from a solo flight of the towing aircraft with smoke-generating cartidges mounted on both wing tips. A subsequent untethered loose formation flight of the two aircraft was used to study the effects of the flow field from the towing aircraft (including downwash, engine exhaust, and wing tip vortices) on the towed aircraft in the selected tow positions. Flight results showed that the flow field effects were negligible and could be ignored in the simulation.

Aircraft Simulation

The mathematical model of the towed aircraft was based on a full-envelope, nonlinear, piloted simulation of the F-106 airplane at NASA Langley Research Center, Hampton, Virginia (ref. 17). The force and moment terms in the equations of motion were augmented by the contribution of the towrope tension, which are shown schematically in figure 11. The simulation used the simplifying assumption that the towrope tension acted along the line-of-sight between the attach points on the two aircraft. The elevation and azimuth angles of the towrope with respect to the body axes of the towed aircraft were determined from the direction cosines of the towrope tension vector.

The low-speed portion of the aerodynamic database incorporated in the simulation is described in reference 18. In addition to the complete aerodynamic characterization, the simulation included surface actuator dynamics, a mathematical model of the turbojet engine with afterburner, landing gear dynamics, ground effect, atmospheric wind, and turbulence. The simulation was interfaced with a fixed-base generic fighter-type cockpit with a programmable stick force feedback and a simple visual system displaying an earth-sky scene and a generic tow plane. A photograph of the towed aircraft simulator cockpit and visual scene is shown in figure 12. The tow plane image visible in the photograph was generated by a trajectory of a separate generic transport airplane simulation. Initially, the tow plane trajectory was generated independently from the towed aircraft simulation. Each time point on the trajectory was used in the towed aircraft simulation to establish the direction and magnitude of the tension

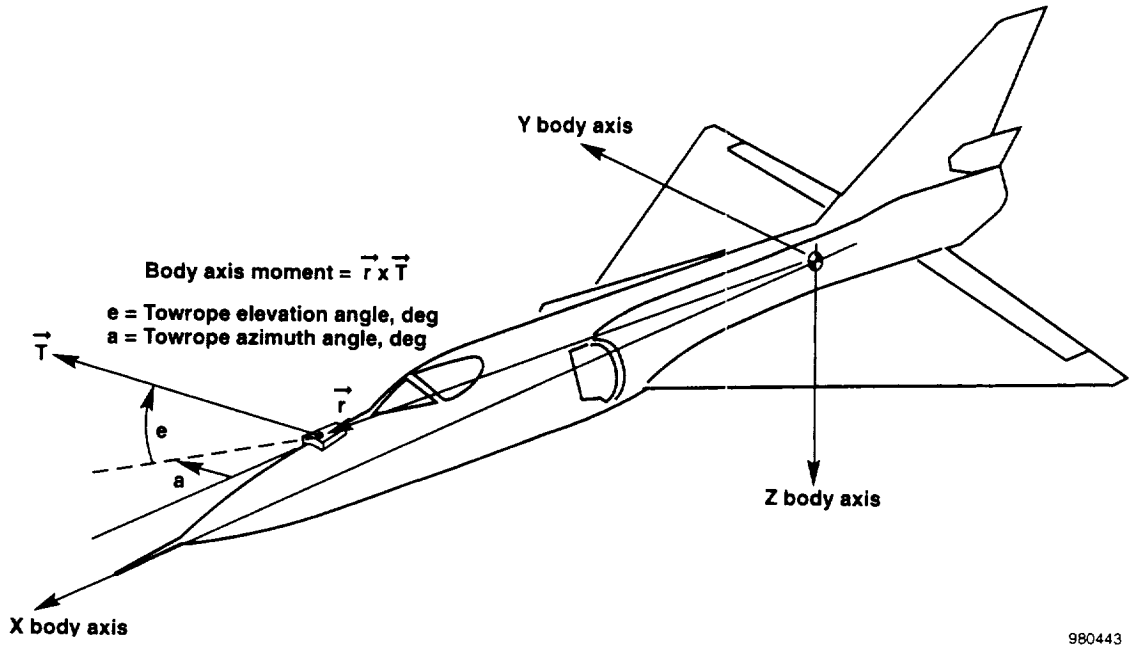

Figure 11. Definition of towrope tension vector and moment.

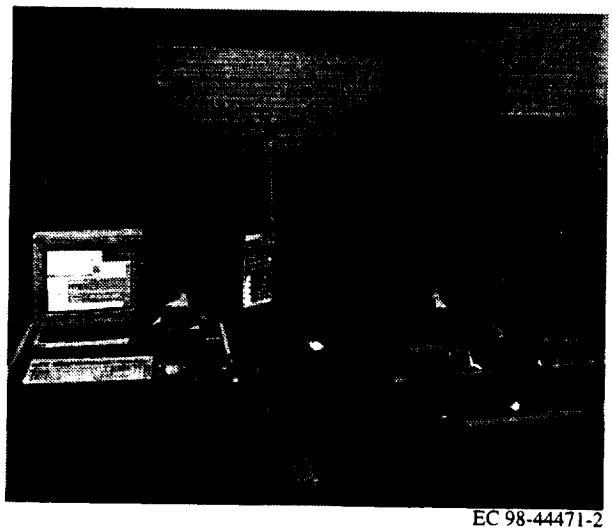

Figure 12. Piloted simulation cockpit and visuals.

vector and to drive the tow plane visual display. Later, the low-speed aerodynamics, mass, inertia, and propulsion system characteristics of the towing aircraft were incorporated in a transport airplane simulation. Eventually this simulation also incorporated the towrope forces and moments so that the two simulations could be operated simultaneously with the necessary data exchange taking place through a fiber optic reflected memory. Through the use of this combined simulation it was possible to justify the assumption that in normal towed flight the effect of the towed aircraft on the towing aircraft dynamics is negligible. This result was expected because the mass ratio of the two aircraft was approximately 1 to 6.

Towrope Model

The towrope was analytically modeled as a straight, extensible nonlinear spring-damper system. Documented stiffness and damping properties were unavailable for the towrope; laboratory testing described in the Ground Testing section was used to experimentally determine these properties. Figure 13 shows the load-elongation curve resulting from a cyclic-loading test case with minimum tension of 3000 lb, maximum tension of 24,000 lb, and a time period of 5 sec. The positive curvature shows that the rope has the characteristic of a stiffening spring. The difference between the loading portion of the curve and the unloading portion of the curve shows the mechanism by which the rope absorbs energy and provides damping (ref. 19).

The elongation response of an analytical spring-mass-damper system was computed using the same cyclic-loading input used in the laboratory tests. The coefficients of spring stiffness and damping were adjusted until the computed solution closely agreed with the load-elongation laboratory test data. A model that was second-order in spring stiffness and first-order in viscous damping was found to capture the essential characteristics of the physical system.

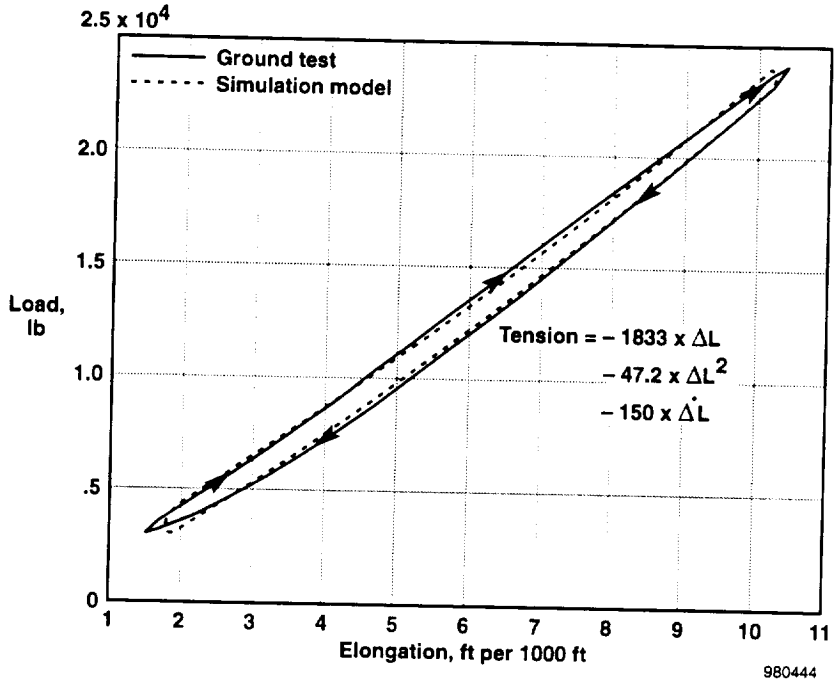

Figure 13. Load-elongation test results for towrope.

The computed (i.e. simulated) load-elongation curve is overlaid on the corresponding laboratory-test load-elongation curve in figure 13. The model coefficients used in the computed solution and implemented in the piloted simulation are also shown in the figure.

Trim Prediction

For aircraft in untethered flight at a given altitude, the longitudinal trim solution is uniquely specified by the elevator deflection, angle of attack, and airspeed. For the towed configuration the trim solution is augmented with the additional variables of tow tension and towrope elevation angle (or alternatively the horizontal and vertical separation between the two aircraft). Two separate trim solutions were computed; one using the assumption implemented in the real-time piloted and batch simulations that the towrope was straight (straight-rope trim solution), and one allowing for curvature of the towrope (rope-sail trim solution). The straight-rope trim solution was computed using either the real-time or the batch simulation, and the offline rope-sail trim solution was computed using a combination of the straight-rope trim solution and additional offline computations. Only the vertical and horizontal separations changed between the straight-rope and the offline rope-sail trim solutions.

The built-in automatic trimming feature (autotrim) of the simulation was used to compute the straight-rope trim solution. Vertical separation was specified and the autotrim feature computed the elevator deflection, angle of attack, towrope tension, and towrope elevation angle required to hold the aircraft in trimmed flight.

Using trim conditions at the towed aircraft from the straight-rope trim solution, the offline rope-sail trim solution was computed by approximating the continuously-curved towrope with a large number of discrete, straight-rope segments. Beginning at the towed aircraft, stepwise application of force-balance equations for each rope segment up to the forward end of the rope yielded the trim solution for the rope shape (ref. 9 and 15). The height of the forward end of the rope emerged as the vertical separation for the offline rope-sail trim solution.

Stability Prediction

The batch simulation had provisions for linearizing around a trimmed, straight flightpath at a selected flightpath angle. The resulting linear system of differential equations allowed an evaluation of stability with various vertical separation distances, towrope characteristics, and flightpath angles. The roots of the characteristic equations for the longitudinal and lateral-directional linear differential equations are shown in figures 14 and 15 for values of vertical separation ranging from 100 to 500 ft. The towed aircraft is at an indicated airspeed of 190 kn in level flight at an altitude of 10,000 ft and below the towing aircraft (in the

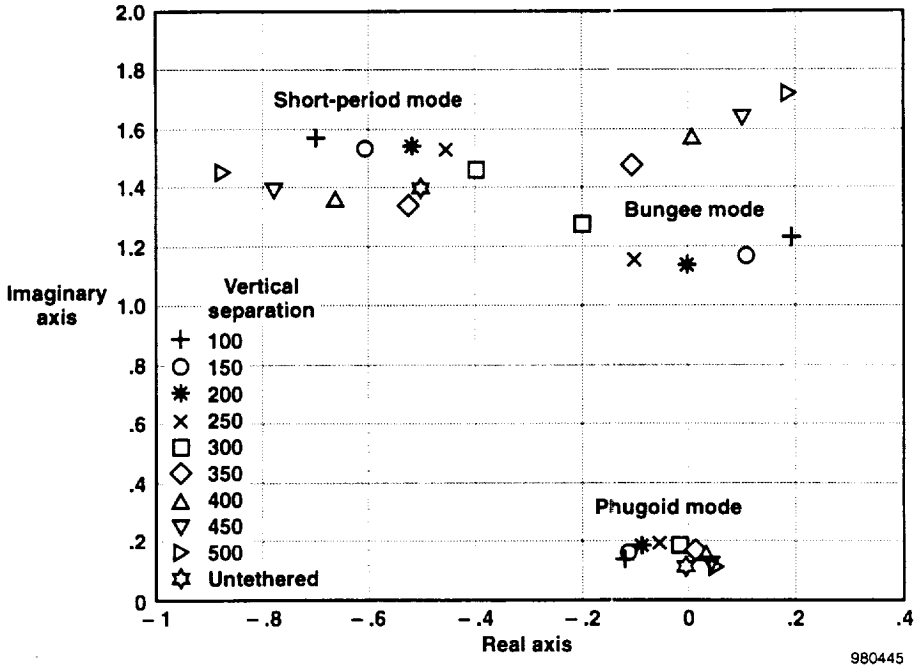

Figure 14. Simulation prediction of effect of vertical separation on longitudinal stability.

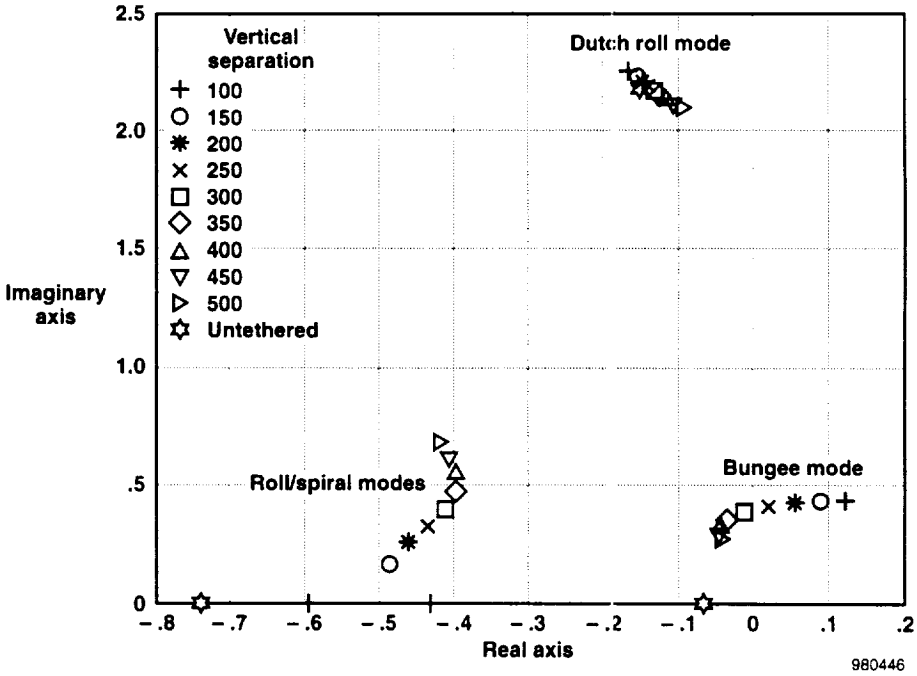

Figure 15. Simulation prediction of effect of vertical separation on lateral-directional stability.

low-tow position). In each figure three oscillatory modes are present and it is clear that the vertical separation has a strong effect on all modes. In fact, the bungee mode is predicted to be stable only in a 100-foot-wide band between 300 and 400 ft below the tow plane. Another noticeable effect of towing is the merging of the spiral and roll modes into a heavily damped oscillatory mode. More than approximately 320 ft below the tow plane, the phugoid mode exhibits a slight instability. For reference, the untethered roots are also shown in the figures 14 and 15. In the pitch axis, these roots are located close to the modified short-period and phugoid roots at the 300- to 400-ft tow separation. In the lateral-directional axes, towing is seen to have a minor effect on the dutch roll mode, but a strong effect on both the spiral and roll modes. Subsequent portions of this paper show that these predictions of the linear system were not always borne out by the results of the flight tests, principally because of the assumption that the towrope remains straight at all times.

Flight Test Preparation and Operation

Prior to towed flight operations, both aircraft were equipped with research instrumentation systems. Critical operational procedures were developed using the simulator and other processes. The following sections discuss in detail the preparation of the aircraft and development and implementation of the operational flight plan for the research missions.

Instrumentation

Both test aircraft were equipped with research instrumentation systems. The towed aircraft had a complete suite of conventional aircraft instrumentation, including airdata (airspeed, altitude, Mach number, angle of attack, angle of sideslip), linear accelerometers (two independent 3-axis packages), angular rates (one 3-axis package), Euler angles, control surface positions (rudder and both elevons), voltage monitors, and a number of discretes (gear, speedbrake, etc.). The aircraft also had additional test-specific instrumentation installed, including tow tension (two independent measurements), and tow elevation and azimuth angles. All instrumentation was ground-calibrated prior to flight operations. In flight, all of the measurements were telemetered to the ground for real-time monitoring in the control room and for permanent recording. Additionally, the tow tension measurements were available to the pilot on a cockpit display.

The towing aircraft also had a complete suite of conventional aircraft instrumentation, including airdata (airspeed, altitude, Mach number), inertial navigation system (linear accelerations, velocities, position, angular rates and Euler angles), control surface positions, and engine pressure ratios and speeds. In flight, all of the measurements were recorded on magnetic tape for permanent storage and were postprocessed on the ground.

Each aircraft was equipped with a 12-channel carrier-phase differentially-corrected global positioning system (DGPS) receiver-recorder unit. In flight, the data from each receiver-recorder was logged internally. After each flight, the logged data was postprocessed using carrier-phase differential corrections from a ground base station. The data sets from the four separate systems were time-synchronized and merged into a single data set for analysis.

Development of Flight Test Procedures

The simulation was used to formulate and validate flight test procedures prior to flight. This was true for both normal and emergency scenarios. In fact, on one occasion all of the critical displays in the ground control room were connected to the dual simulator configuration so that the test team could rehearse many different flight scenarios involving both aircraft. Inadvertent towrope release at low altitude and low airspeed was of particular concern; hence, this was simulated many times. This use of the simulator was validated early in the test program in solo flights of the towed aircraft by the project pilot while performing wave-offs from low altitudes at idle power settings. Other typical uses of the simulation included (1) the examination of towrope tension in the various phases of towed flight, including takeoff roll, (2) examination of trim conditions at different vertical separation distances, (3) prediction of takeoff distances of the two aircraft, (4) evaluation of the effect of atmospheric turbulence on the towed aircraft while on tow, and (5) the assessment of landing gear load during the takeoff roll. These studies were conducted either in the piloted or the unpiloted (batch) version of the full nonlinear simulator. In most cases it was satisfactory to use the towed aircraft simulation alone with a 'canned' towing aircraft trajectory.

Typical Flight Operation Scenario

Smooth flight operations were developed through practice. Both aircraft were initially positioned on the taxiway and the tow train was connected to the towed aircraft. After engine startup and other preflight checks, both aircraft were taxied to predetermined positions on the runway. The towed aircraft throttle was left at an idle power setting throughout the remainder of the towed operation; this provided the towed aircraft with

hydraulic power, electrical power, and safety abort capability. The tow train was unrolled from its storage spool and connected to the towing aircraft. All ground operations crew were removed from the runway, the brakes were locked on the towed aircraft, and the towing aircraft moved forward to set the towrope tension to about 6000 lb and raise the tow train off the runway surface. The towing aircraft released its brakes and slowly throttled up to a predetermined power setting. As the tension rose, the brakes of the towed aircraft were gradually released to manage tow tension.

The towing aircraft accelerated, rotated at about 105 kn calibrated airspeed (KCAS), lifted off at about 115 KCAS, and began its climb out while accelerating to 190 KCAS. The towed aircraft stayed on the ground until its rotation at about 120 KCAS and its takeoff at about 165 KCAS. The aerotow system ascended to a typical test condition of 10,000 ft. altitude and 190 KCAS, where on-tow flight test maneuvers were executed. At conclusion of the on-tow test points, the towed aircraft released the tow train and returned to base. The towing aircraft descended to about 2,700 ft above ground level, released the tow train over a designated drop zone, and returned to base.

Flight Test Points

The flight test program consisted of several untethered flights of both aircraft, one high-speed taxi test of the towed configuration, and six tethered flights. The untethered flights were used to check the functionality of the modified and instrumented towed aircraft, to perform calibrations of the towed aircraft airdata system, to establish a baseline on the takeoff performance of the towing aircraft, and investigate the effect of the towing aircraft engine, tip vortex, and body wake on the towed aircraft. The untethered flights also included trim points, pitch and roll-yaw doublet maneuvers, and idle-power descent test points for evaluating the trim, stability, and performance modeling of the baseline towed aircraft simulation. The high-speed taxi test was used to validate the takeoff performance and tow tension modeling of the towed configuration. The towed flights were flown within a fairly limited flight envelope; after takeoff the towed configuration accelerated to, and spent the remainder of the flight at, 190 KCAS. After initial climbout, most test points were flown between an altitude of 5000 and 10,000 ft, although the final flight was towed to an altitude of 24,500 ft.

Early towed missions were flown with a nylon damper in the tow train and the towed aircraft in a high-drag or dirty (landing gear down and speedbrake open) configuration. Later missions were flown with no nylon damper in the tow train and the towed aircraft in a low-drag or clean (landing gear up and speedbrake closed) configuration.

The majority of the test points were flown to collect flight data to evaluate the predictive capability of the towed system. Trim points over a wide range of parametric variations—drag (both clean and dirty configurations), climb rate (climbing, level flight, descending), vertical separations, lateral offsets, and bank angles (from wings-level up to 45°)—were used to collect flight data to evaluate preflight trim predictions. At a subset of these trim points, pitch and roll-yaw doublets were executed to evaluate the preflight stability predictions. A handling qualities task was also executed at a subset of the trim points.

Additional flight test points flown included turn reversals for handling qualities assessment, intentional probing of the body wake of the towing aircraft by the towed aircraft, pitch doublets executed by the towing aircraft, and intentional overload failures of the frangible link.

Flight Test Results and Comparisons With Predictions

The flight test program generated a large set of engineering data and pilot assessment of the towed system. The following sections present representative flight test results and compare them with preflight predictions where applicable.

Comparison of Flight Data With Ground Test Data for Rope Model

Flight validation of the towrope load-elongation model was possible as a result of including DGPS data collected onboard both aircraft. Given the spatial position and orientation of each aircraft, the straight-line distance between the two attach points was readily computed. Using this straight-line distance to approximate rope length, the approximate elongation of the rope was also readily computed. For a flight test maneuver with a significant excursion in towrope tension, a plot of tension as a function of approximate elongation yields an approximate load-elongation curve for comparison with laboratory test data.

The flight data sets were searched for a single cycle of the bungee mode for which the minimum and maximum tension values most closely matched those of one of the laboratory test cases; a close match was found for minimum and maximum tension values of 3000 and 16,000 lb, respectively. Figure 16 compares the

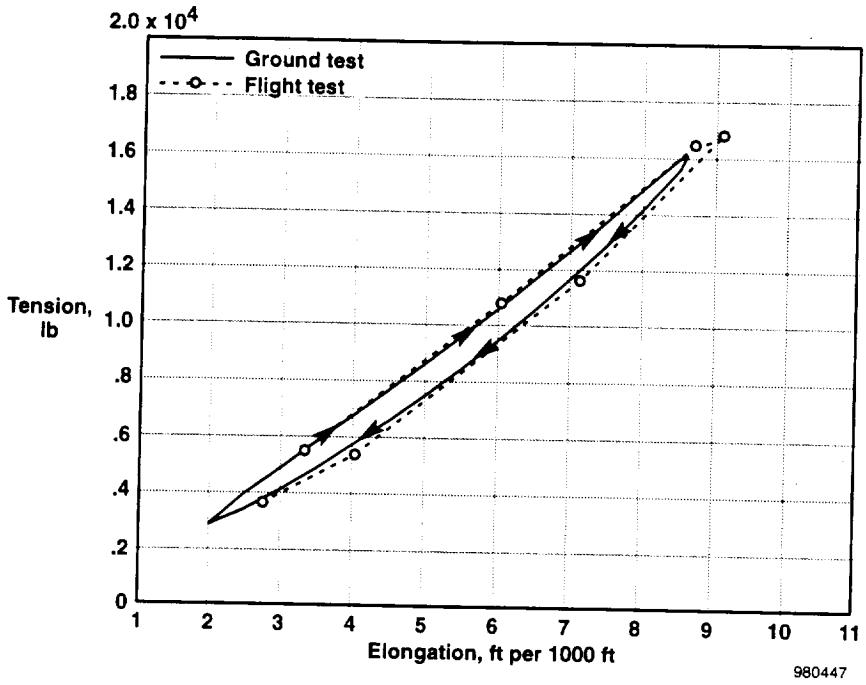

Figure 16. Ground-to-flight comparison of towrope load-elongation curve.

laboratory-derived load-elongation curve with the flight-derived approximate load-elongation curve. The laboratory test data points are of much higher density than the flight data because the laboratory test data are recorded at a high sample rate. The flight data points are limited to 2 samples per sec by the inherent bandwidth limitation of the DGPS data set. It is serendipitous that the bungee mode has a frequency so low (approximately 0.25 Hz) that even low-bandwidth DGPS data are able to capture several independent samples over one cycle.

The flight-derived curve compares favorably with the laboratory-derived curve. All primary characteristics of the rope model—the slope, the curvature, and the separation between the loading and unloading portions of the curve—correlate well between laboratory and flight tests.

Comparison of Flight Data With Simulator Data

Because of the large number of variables involved, the analysis of the towed flight data is a difficult task. At the time of this writing the analysis is still at a preliminary stage; hence, conclusions presented herein are also preliminary. A major contributor to the understanding of the dynamics of towed flight is the validation of the simulator. This work has also just begun, so that the comparison of simulator prediction with towed flight data uses the aerodynamic database and the mathematical model of the towrope without the benefit of new information gathered from the six towed flights.

Untethered Configuration

An effort was made to compare the simulator response with the response of the full-scale airplane to identical control inputs at identical flight conditions. In Figures 17 and 18 the responses of the untethered test airplane are compared with the corresponding responses of the nonlinear simulator at the flight condition of an altitude of 5000 ft and an airplane weight of 33,800 lb. As shown in figure 17, the simulator reproduced the trim angle of attack, elevator position, and pitch attitude within one-half a degree. The dynamic response of the simulator, reflected in the time histories of the principal longitudinal response variables, is also quite satisfactory. The simulator is less accurate in reproducing the lateral-directional response of the real airplane as shown in Figure 18. Although both the aileron and rudder effectiveness are similar to those measured in flight, the dutch roll frequency of the airplane is lower, and the damping is higher than that of the simulator.

Towrope Tension

One of the important uses of the simulator was the prediction of towrope tension. The overall experience with the simulator in this area was satisfactory. At no

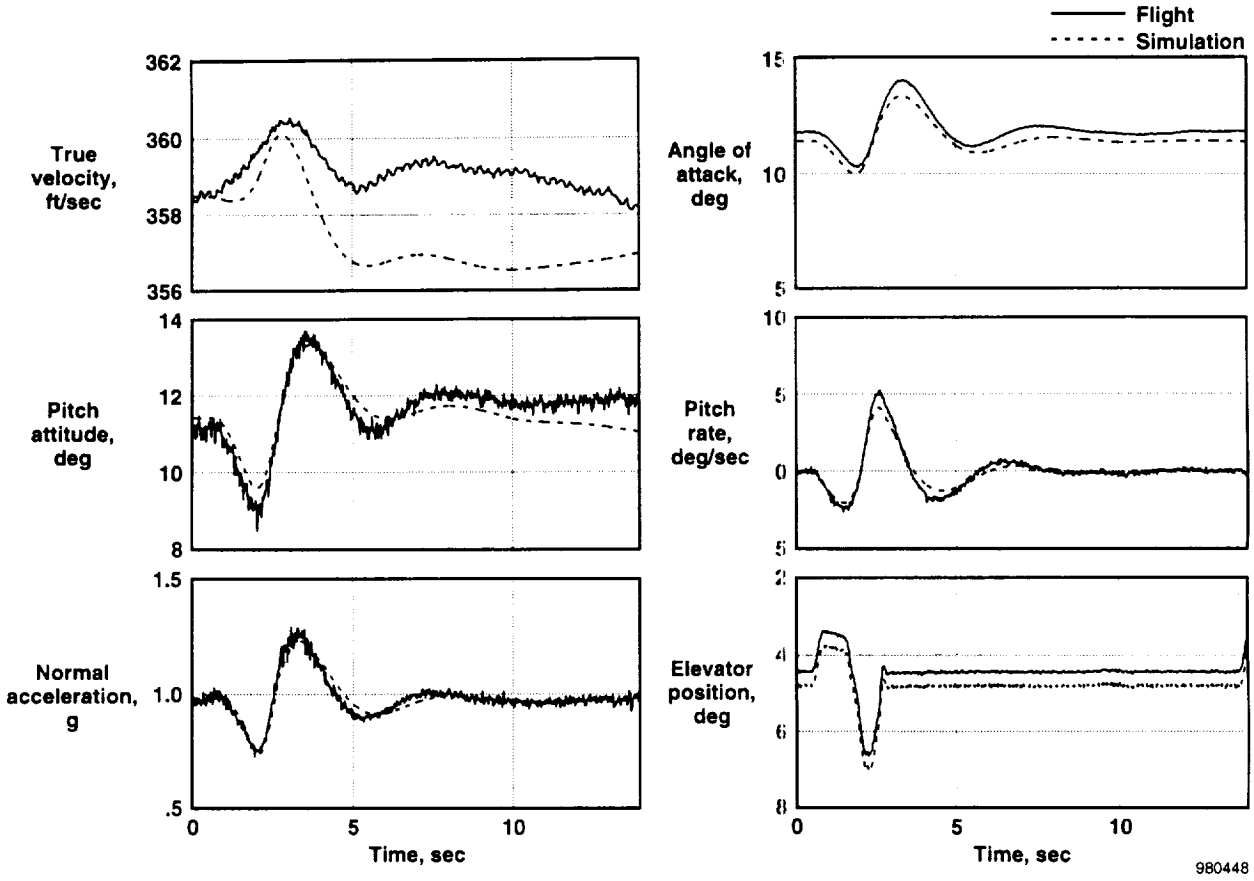

Figure 17. Simulation-to-flight comparison of longitudinal response to a pitch doublet in untethered flight.

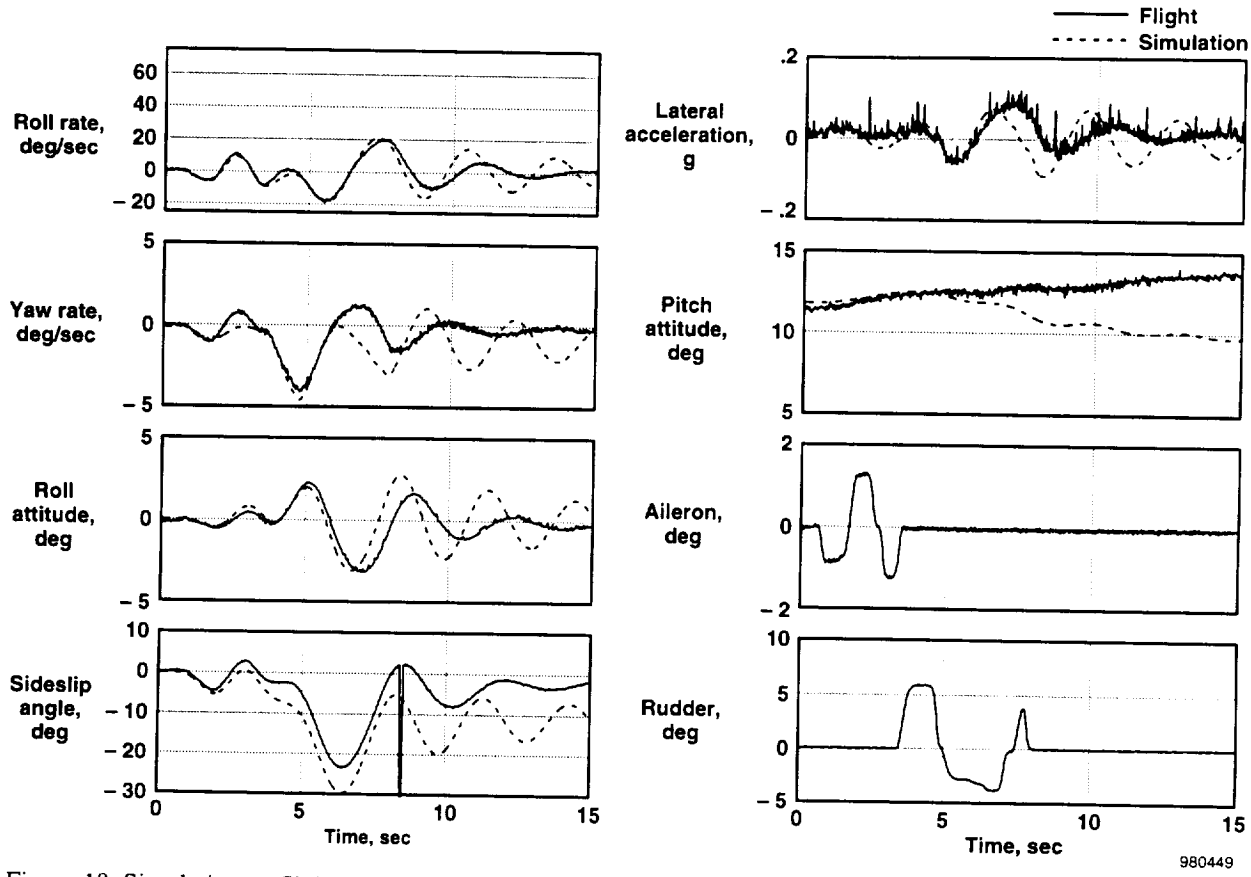

Figure 18. Simulation-to-flight comparison of lateral-directional response to a roll-yaw doublet in untethered flight.

time during the test program did the simulator underpredict the towrope tension; in fact after the first few flights it was noticed that the towrope tension was overpredicted by approximately 2,000 lb in up-and-away flight in all flight configurations. In figure 19 a relatively long 3-minute time segment is shown. Time history of the towrope tension is shown at the top of the figure, while in the middle the landing gear and speed brake states are shown. The continuous, approximately 0.25 Hz oscillation in the towrope tension is the bungee mode that was excited by the longitudinal and lateral-directional doublets (which are not shown in the figure). The vertical separation of the two aircraft, approximately 230 ft, is shown in the lower part of figure 19. Although the bungee mode was lightly damped at this condition, the average values of the towrope tension are readily observable. These values are listed in table 1, next to the simulator predictions as a function of the airplane configuration:

As table 1 shows, the amount of overprediction is approximately 2,000 lb. The wind tunnel drag data in reference 18 and the results of idle-power timed glides

Table 1. Towrope tension variation with flight configuration.

Towrope tension		Configuration	
Flight average, lb	Simulator, lb	Gear	Speedbrake
5,200	7,390	down	in
6,900	9,150	down	out
4,900	6,900	up	out
3,200	5,150	up	in

were examined to assess the actual drag of the towed aircraft. These data indicated that the simulation had excessive drag at the flight conditions where most of the tow tests were performed, i.e., below a dynamic pressure of 130 lb/ft^2. Once this drag discrepancy was identified, satisfactory predictions of the towrope tension could be obtained by advancing the simulator throttle setting to cancel the approximately 2,000 lb of excess drag.

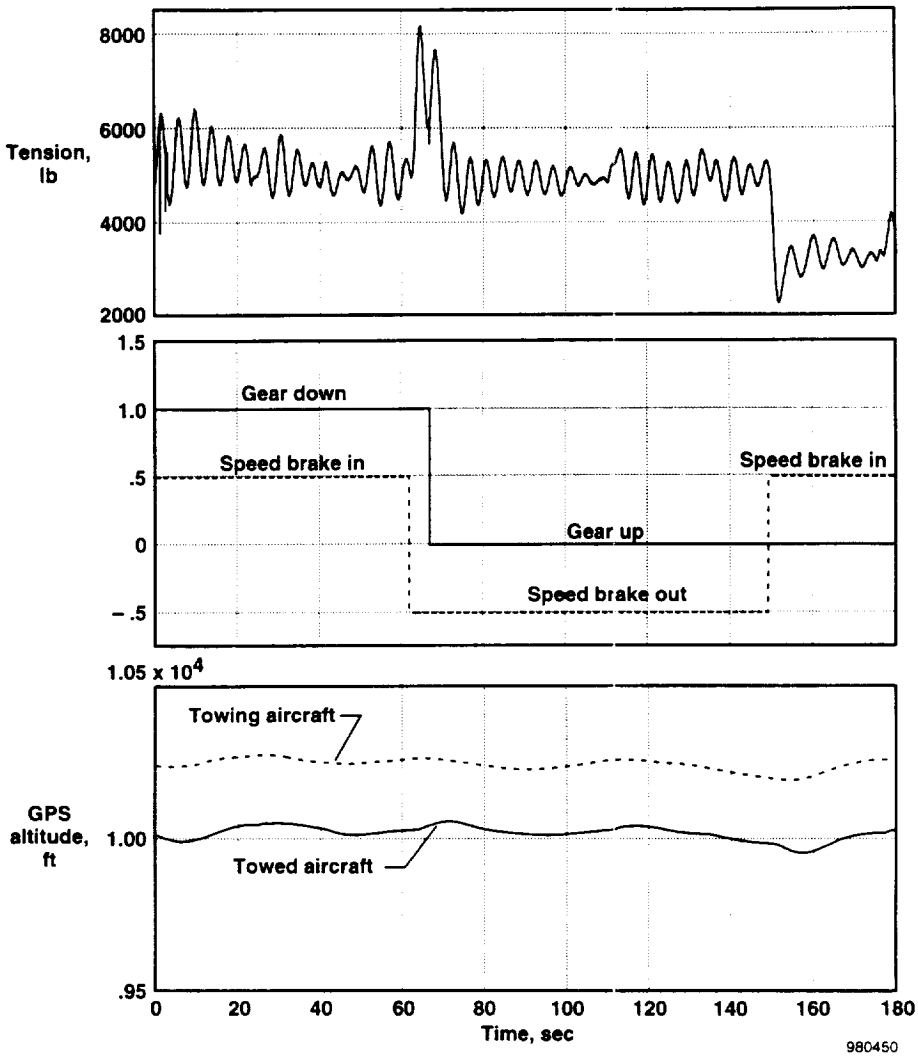

Figure 19. Effect of configuration change on tow tension.

Trim of Tethered Configuration

In flight it was apparent that the static (i.e. trimmed) rope shape was a function of the tension and the vertical separation between the two aircraft. For small vertical separations the trim shape was bowed downward and for large vertical separations the trim shape was bowed upward; between the two extremes there typically was a point at which the rope was essentially straight. Figure 20 shows the rope shape from the towing aircraft for a test point at large vertical separation.

Comparisons of the trim prediction (both the straight-rope and rope-sail models) and the flight test points were categorized by drag configuration for clarity. For the following comparisons the throttle setting was advanced to 17.9 percent (corresponding to 2,382 lb thrust) to correct for the drag discrepancy in the simulation. Figure 21 presents comparisons for the clean configuration and figure 22 presents comparisons for the dirty configuration; the scales for both figures are identical. Each figure contains four subplots: (a) elevator deflection, (b) angle of attack, (c) rope elevation angle at the towed aircraft, and (d) towrope tension, each plotted with vertical separation as the independent variable. Each subplot contains two curves corresponding to the straight-rope and the offline rope-sail trim predictions, as well as symbols corresponding to the flight data points.

When looking at these subplots (fig. 21 and 22), one trend is clear. For both the clean and dirty drag configurations, the offline rope-sail model yields a much better prediction of the in-flight trim than does the straight-rope model.

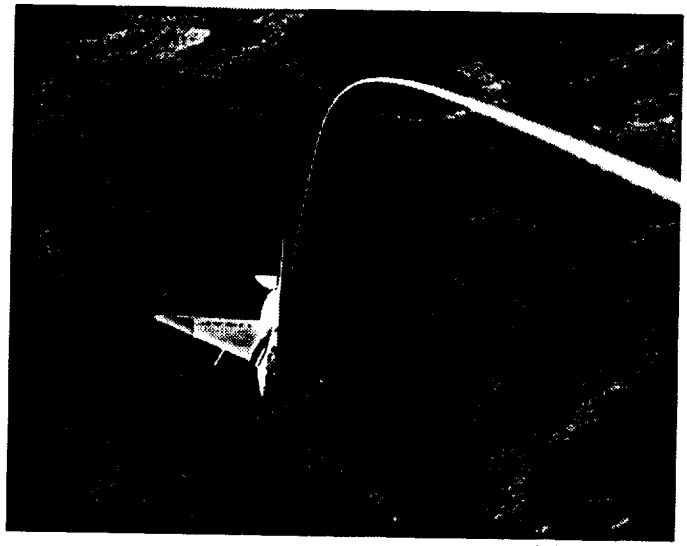

EC98-44393-52

Figure 20. View of towed aircraft and towrope shape from towing aircraft.

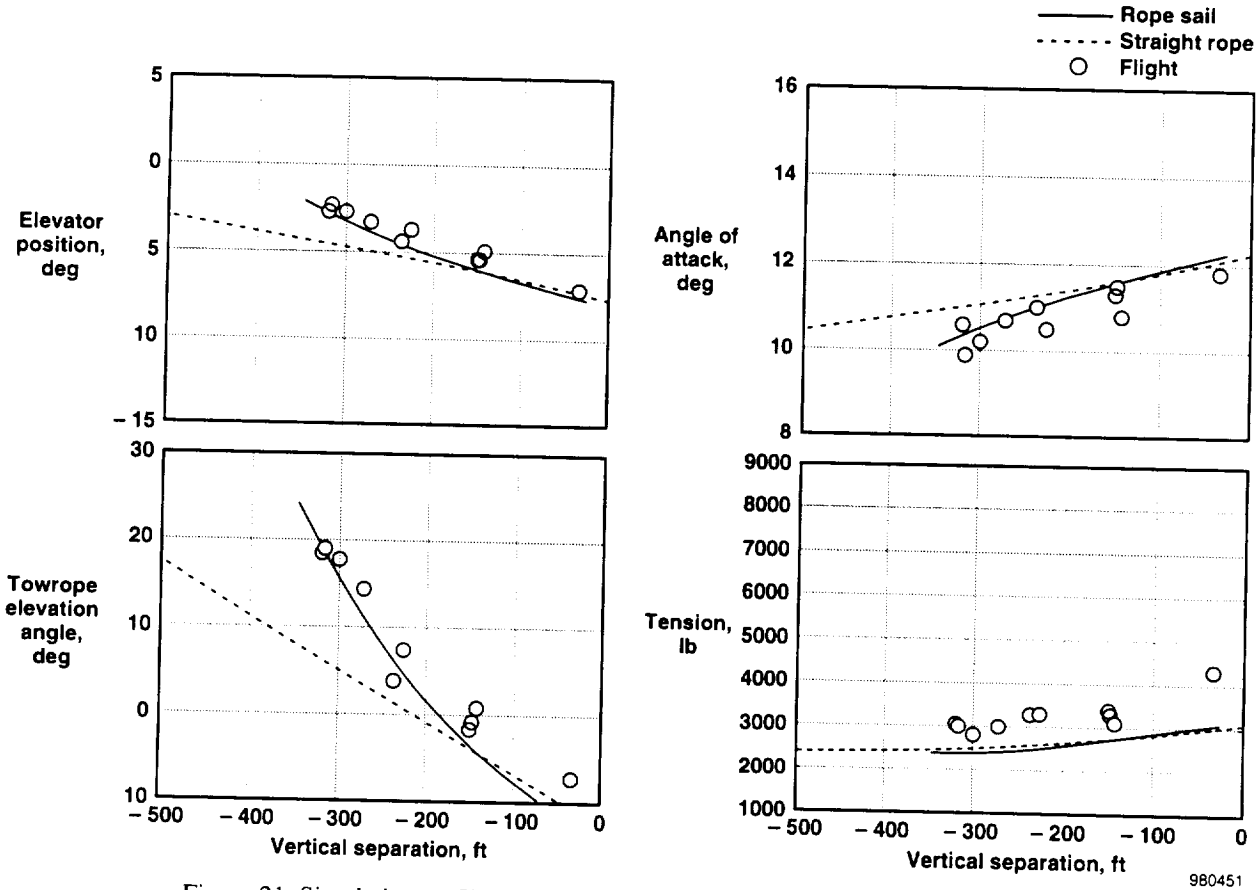

Figure 21. Simulation-to-flight comparison of trim solution in clean configuration.

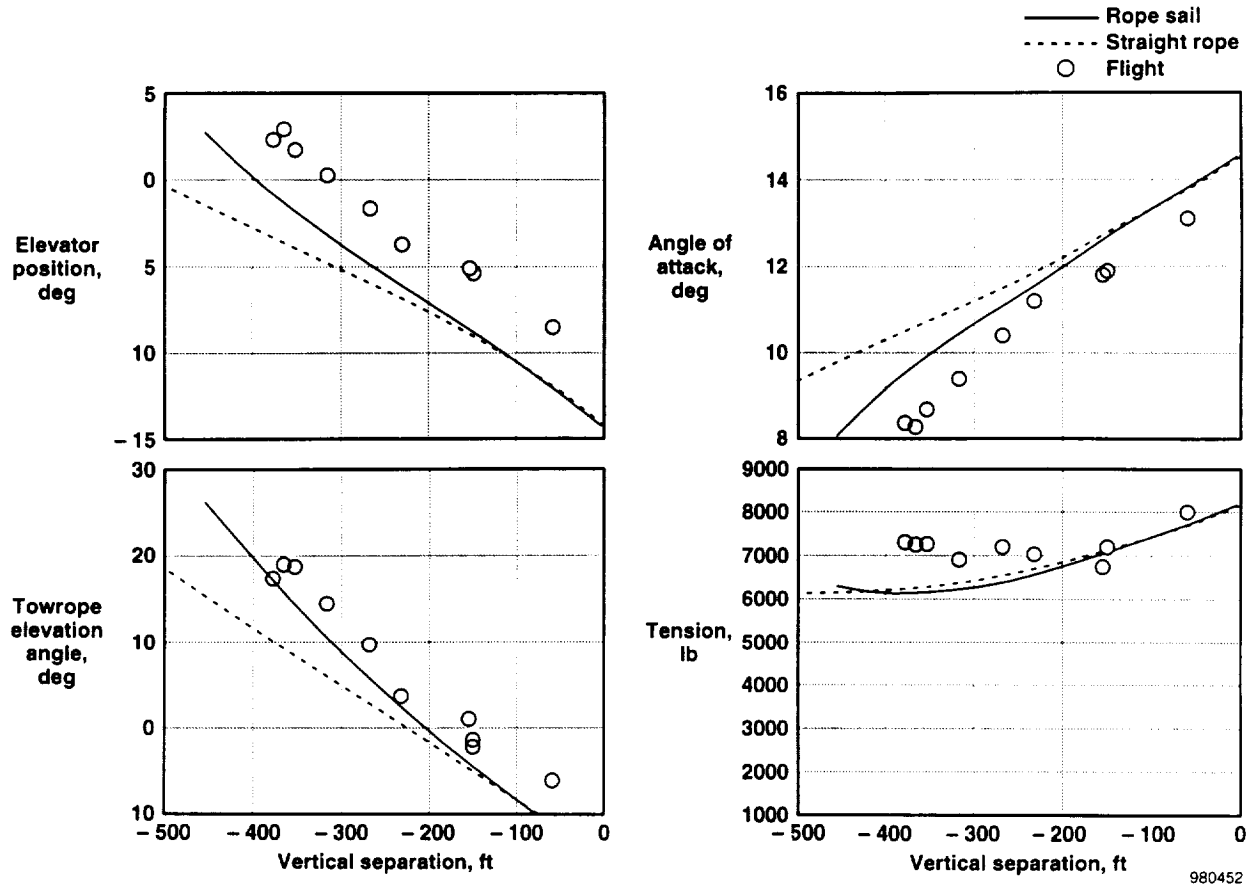

Figure 22. Simulation-to-flight comparison of trim solution in dirty configuration.

When comparing the clean configuration with the dirty configuration, three general trends are clear. The flight-to-simulation comparisons of trim elevator and trim angle-of-attack are better across the board for the clean configuration; for the dirty configuration the simulation underpredicts trim elevator deflection and overpredicts trim angle-of-attack. For the dirty configuration, elevator deflection and angle of attack also show a greater sensitivity to vertical separation than they do for the clean configuration. This greater sensitivity occurs because the dirty configuration requires larger elevator deflection increments to trim out the larger pitching moment resulting from the larger trim tension values. Conversely, for the clean configuration the rope elevation angle shows a greater sensitivity to vertical separation than it does for the dirty configuration. Lower tension values associated with the clean configuration allow the rope sail associated with the aerodynamic forces to show an increased influence. For both the clean and dirty configurations, the simulation underpredicts the tension values by approximately 600 to 1000 lb when the throttle is advanced to account for the drag discrepancy.

Dynamics of Tethered Configuration

In figure 23 the longitudinal response of the towed aircraft is compared with the response of the simulator at the identical initial flight conditions, at an approximate altitude of 10,000 ft and a true airspeed of 376 ft/sec. The towed aircraft was in the dirty configuration. Vertical separation between the two aircraft was approximately 330 ft initially, and varied less than ±25 ft during the time interval of 15 sec. The flight-measured pitch doublet was added to the simulator trim elevator setting.

In comparing the trim values first, as shown during the initial portion of the time histories, note that the trim angle of attack, and pitch attitude agree with each other, as was also true for the untethered flight case (fig. 17). In flight approximately 3° more nosedown elevator was required to balance the more positive pitching moment caused by the larger positive initial towrope angle. With the exception of the angle-of-attack responses, the simulator reproduced the initial (i.e. forced) response of the towed aircraft. The frequency of the response was

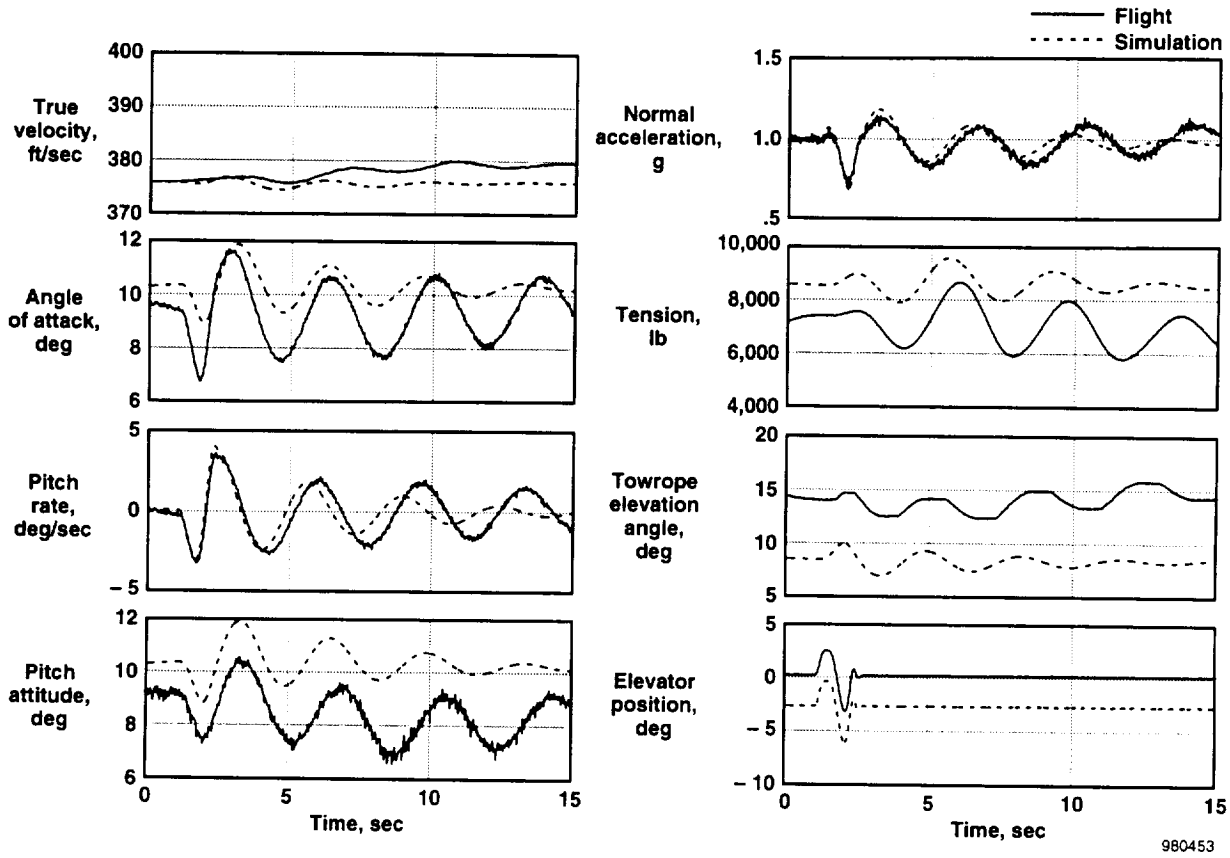

Figure 23. Simulation-to-flight comparison of longitudinal response to pitch doublet in towed flight.

accurately reproduced by the simulator, though the damping in flight was lower than that of the simulator. The difference between the angle-of-attack response of the aircraft and the simulator is not fully understood. In this example the longitudinal short period mode and the bungee mode are indistinguishable from each other.

The overall longitudinal response at the 330-ft vertical separation is considerably different from the untethered response, undoubtedly as a result of the towrope tension and the orientation of the towrope tension with respect to the towed aircraft. It should be noted from this figure (fig. 23) that the towrope elevation angle measurement is indicating a strong nonlinearity by the flattened peaks of the sinusoidal oscillations. The source of the nonlinearity is more likely found in friction at the universal joint than in the dynamics of the towrope itself.

Figure 24 shows that the agreement of the lateral-directional responses between flight and simulation is less favorable, just as it was for the untethered flight. Although the amplitude and the damping of the flight and simulator data are similar, the flight data shows lower frequency. Considering the simulator data alone, the oscillations in the simulator towrope tension damp out after two cycles. This result indicates the presence of a lateral-directional bungee mode and that this mode has higher damping than the simulator dutch roll mode. The towrope azimuth angle measurement trace exhibits a nonlinearity similar to that observed in the longitudinal case (fig. 23).

Handling Qualities Evaluations

A limited number of handling qualities evaluations were performed in both the clean and the dirty configuration. The evaluation task consisted of aggressive reacquisition of the centerline position behind the towing aircraft from a lateral offset that was approximately in line with one of the outboard engines of the towing aircraft. This amount of lateral offset required a considerable amount of roll-stick and rudder-pedal deflection by the pilot of the towed aircraft. The offset also resulted in approximately one-quarter ball deflection on the tow plane bank indicator. For reference, the same task was also performed off-tow.

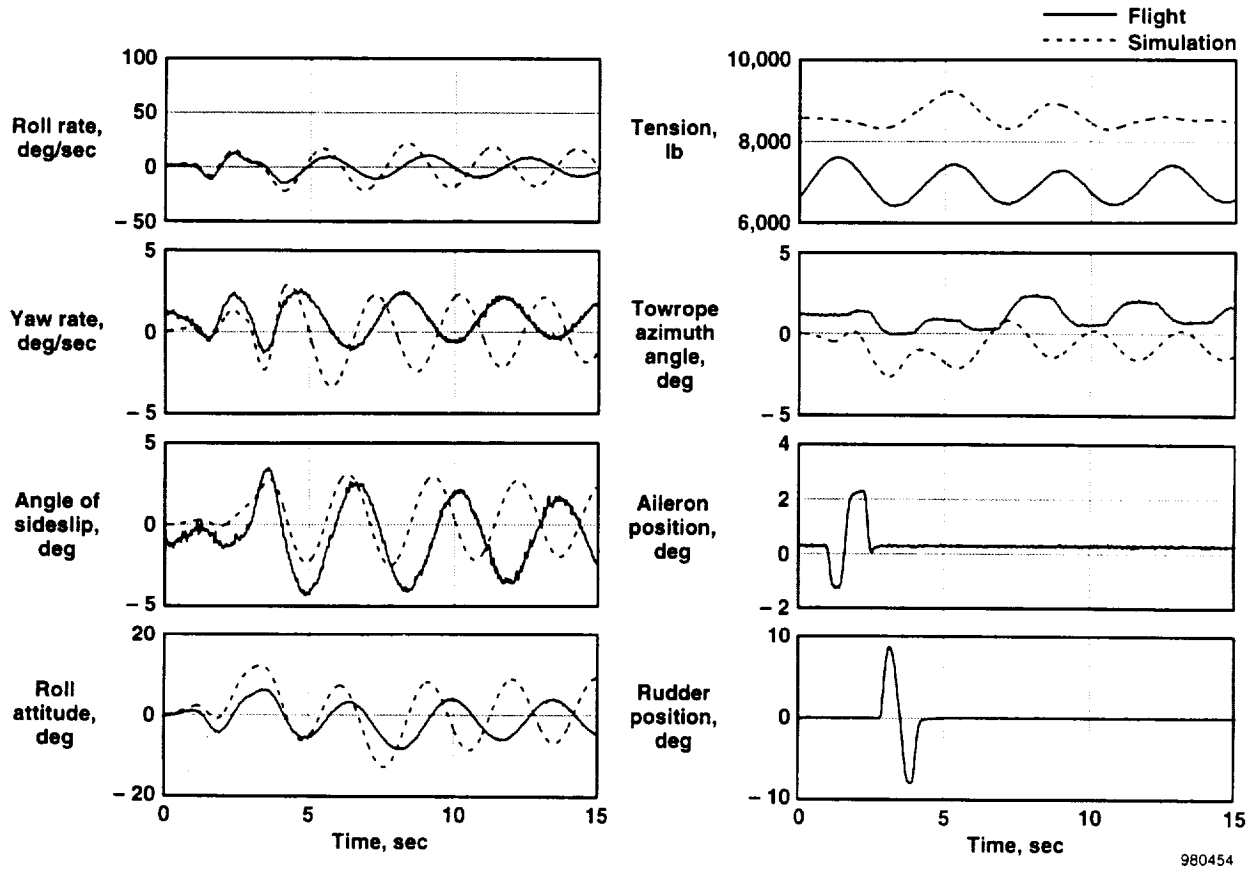

Figure 24. Simulation-to-flight comparison of lateral-directional response to roll-yaw doublet in towed flight.

The pilot of the towed aircraft rated the task on the Cooper-Harper rating scale (ref. 20) during towed flight as a rating of 2 in both the clean and the dirty configuration. Off-tow a pilot rating of 3 was given to the task. The pilot commented that the task was easy to perform in all configurations, with the on-tow, dirty configuration being the easiest. While on-tow, the pilot only had to relax the controls to reacquire the centerline position, in contrast with the off-tow task during which aggressive control inputs were required to return to the centerline.

Pilot comments, in general, indicated that in the normal tow position, that is between 200 and 300 ft below the tow plane, the towed aircraft was 'easy' and 'pleasant' to fly in level, as well as climbing or descending flight. The maximum climb rate tested was 2,000 ft/min; the rate of descent was limited to 1,000 ft/min, especially in the clean configuration, to prevent excessive towrope slack.

Concluding Remarks

A flight test program demonstrated the feasibility of aerotow of a space launch configuration by a transport-class aircraft Use of existing aircraft, structural components, analytical structural modeling, and extensive ground testing produced a robust aerotow system. Structural modifications to the towing aircraft and the towed aircraft proved to be entirely adequate to carry the tow-induced structural loads. Prior to towed flight operations, loose formation flying demonstrated the influence of the tow plane flow field (including downwash, engine exhaust, and wing tip vortices) on the towed aircraft to be minimal. Preflight simulations were used to develop standard and emergency operational procedures, and identified important characteristics of the aerotow system.

Comparison of flight test results with preflight simulation-based predictions was promising in some aspects and disappointing in others. Takeoff distance and

REPORT DOCUMENTATION PAGE

Form Approved
OMB No. 0704-0188

1. AGENCY USE ONLY (Leave blank)	2. REPORT DATE	3. REPORT TYPE AND DATES COVERED
	September 1998	Technical Memorandum

4. TITLE AND SUBTITLE

An Overview of an Experimental Demonstration Aerotow Program

5. FUNDING NUMBERS

WU 242-33-02-00-25-00-000

6. AUTHOR(S)

James E. Murray, Albion H. Bowers, William A. Lokos, Todd L. Peters, Joseph Gera

7. PERFORMING ORGANIZATION NAME(S) AND ADDRESS(ES)

NASA Dryden Flight Research Center
P.O. Box 273
Edwards, California 93523-0273

8. PERFORMING ORGANIZATION REPORT NUMBER

H-2279

9. SPONSORING/MONITORING AGENCY NAME(S) AND ADDRESS(ES)

National Aeronautics and Space Administration
Washington, DC 20546-0001

10. SPONSORING/MONITORING AGENCY REPORT NUMBER

NASA/TM-1998-206566

11. SUPPLEMENTARY NOTES

Presented at 30th Anniversary Symposium of the Society of Flight Test Engineers, Inc., September 15–17, 1998, Reno, Nevada. James E. Murray, Albion H. Bowers, William A. Lokos, Todd L. Peters, NASA Dryden Flight Research, Edwards, CA; Joseph Gera, Analytical Services and Materials, Inc., Edwards, California.

12a. DISTRIBUTION/AVAILABILITY STATEMENT

Unclassified—Unlimited
Subject Category ~~36~~ 05

12b. DISTRIBUTION CODE

13. ABSTRACT (Maximum 200 words)

An overview of an experimental demonstration of aerotowing a delta-wing airplane with low-aspect ratio and relatively high wing loading is presented. Aerotowing of future space launch configurations is a new concept, and the objective of the work described herein is to demonstrate the aerotow operation using an airplane configuration similar to conceptual space launch vehicles. Background information on the use of aerotow for a space launch vehicle is presented, and the aerotow system used in this demonstration is described. The ground tests, analytical studies, and flight planning used to predict system behavior and to enhance flight safety are detailed. The instrumentation suite and flight test maneuvers flown are discussed, preliminary performance is assessed, and flight test results are compared with the preflight predictions.

14. SUBJECT TERMS

ECLIPSE, Tethered aircraft, Towed aircraft, Towing aircraft, Towed system stability, Tow rope

15. NUMBER OF PAGES

29

16. PRICE CODE

A03

17. SECURITY CLASSIFICATION OF REPORT	18. SECURITY CLASSIFICATION OF THIS PAGE	19. SECURITY CLASSIFICATION OF ABSTRACT	20. LIMITATION OF ABSTRACT
Unclassified	Unclassified	Unclassified	Unlimited

peak tow tension during takeoff were well-predicted, as was the lack of effect the towed aircraft had on the towing aircraft. Trim tow tension and trim elevator deflection were generally underpredicted and trim angle of attack was generally overpredicted, with the discrepancy increasing as the net drag of the test aircraft was increased. However, the trends in the trim solution as a function of vertical separation were generally well-predicted. For the trim solution, modeling the tow train as a single, straight, elastic element proved inadequate; however, a simple static model of the tow train as a series of connected, straight, elastic elements significantly increased the accuracy of the trim prediction.

The simulation of the aerotow system dynamics under the assumption of a single, straight, elastic tow train element underpredicted the size of the region of longitudinal stability and overpredicted the lateral-directional stability. Handling qualities of the aerotow system in the region of optimal system stability were generally rated by the pilot as 'easy', with the higher drag configurations receiving more favorable ratings.

References

[1]Martin Simons, Letter to the editor of *Australian Gliding*, vol. 46, no. 11, p. 42, Nov. 1997.

[2]Spate, Wolfgang, *Top Secret Bird, The Luftwaffe's Me-163 Comet*, Pictorial Histories Publishing Company, Missoula, Montana, 1989.

[3]Nissen, James M., Burnett L. Gadeberg, and William T. Hamilton, *Correlation of the Drag Characteristics of a Typical Pursuit Airplane Obtained from High-Speed Wind-Tunnel and Flight Tests*, NACA-TR-916, 1948.

[4]Schwartz, Walter, *Long-Line Tow of Aircraft*, Wright Air Development Center Technical Report 53-111, Nov. 1953.

[5]Horton, Victor W., Richard C. Eldridge, and Richard E. Klein, *Flight-Determined Low-Speed Lift and Drag Characteristics of the Lightweight M2-F1 Lifting Body*, NASA TN D-3021, Sept. 1965.

[6]Page, Tom, *American Soaring Handbook 4 - Airplane Tow*, Soaring Society of America, Inc., 1959.

[7]Phillips, William H., *Theoretical Analysis of Oscillations of a Towed Cable*, NACA TN 1796, 1949.

[8]Maggin, Bernard and Robert E. Shanks, *Experimental Determination of the Lateral Stability of a Glider Towed by a Single Towline and Correlation with an Approximate Theory*, NACA RM L8H23, 1948.

[9]Ockels, Wubbo J., Joris A. Melbert, and Alfred L. C. Roelen, "Stratospheric Towed Vehicle Concept," *Journal of Aircraft*, vol. 31, no. 6, pp. 1328–1332, Nov.–Dec. 1994

[10]Cochran, J. E., Jr., M. Innocenti, T. S. No, and A. Thukral, "Dynamics and Control of Maneurverable Towed Flight Vehicles," AIAA-90-2841, *AIAA Atmospheric Flight Mechanics Conference*, Portland, Oregon, August 20–22, pp. 293–304, 1990.

[11]Clifton, James M., Louis V. Schmidt, and Thomas D. Stuart, "Dynamic Modeling of a Trailing Wire Towed by an Orbiting Aircraft," *Journal of Guidance, Control, and Dynamics*, vol. 18, no. 4, pp. 875–881, July–Aug. 1995.

[12]de Matteis, Guido, "Longitudinal Dynamics of a Towed Sailplane," *Journal of Guidance, Control, and Dynamics*, vol. 16, no. 5, pp. 822–829, Sept.–Oct. 1993.

[13]de Matteis, Guido, "A Theoretical Contribution to the Problem of Towplane Upset," *Technical Soaring*, vol. 21, no. 4, pp. 116–121, Oct. 1997.

[14]de Matteis, G. and W. Tamilla, "Stability Augmentation of a Sailplane in Towed Flight," *Aeronautical Journal*, vol. 97, no. 970, pp. 349–356, Dec. 1993.

[15]Etkin, Bernard, "Stability of a Towed Body," *Journal of Aircraft*, vol. 35, no. 2, pp. 197–205, Mar.–Apr. 998.

[16]Kelly, Michael S., "Space Launch Vehicles Configured as Gliders and Towed to Launch Altitude by Conventional Aircraft," U. S. Patent 5,626,310, May 6, 1997.

[17]Brandon, Jay M., Philip W. Brown, and Alfred J. Wunschel, *Piloted Simulation Study of Effects of Vortex Flaps on Low-Speed Handling Qualities of a Delta-Wing Airplane*, NASA TP-2747, Sept. 1987.

[18]Yip, Long P., *Wind-Tunnel Free flight Investigation of a 0.15-Scale Model of the F-106B Airplane with Vortex Flaps*, NASA TP-2700, Mar., 1987.

[19]Steidel, Robert F., Jr., *An Introduction to Mechanical Vibrations, 2nd. ed.*, John Wiley & Sons, 1979.

[20]Cooper, George E. and Robert P. Harper, Jr., *The Use of Pilot Rating in the Evaluation of Aircraft Handling Qualities*, NASA TN-D-5153, Apr. 1969.